

# Absolute length measurement of prismatic bodies with PTB's new double-ended interferometer under the influence of wavefront aberrations

Katharina Rau<sup>1,\*</sup>, Torsten Mai<sup>1</sup> and René Schödel<sup>1</sup>

<sup>1</sup> Physikalisch-Technische Bundesanstalt (PTB), Bundesallee 100, 38116 Braunschweig, Germany

\* Corresponding author: [katharina.rau@ptb.de](mailto:katharina.rau@ptb.de)

## Abstract

Traceability of length measurements to the international system of units (SI) can be realized by using optical interferometry. This paper describes PTB's new double-ended interferometer, which is used to determine the absolute length of prismatic bodies (e.g. gauge blocks) from the analysis of two sets of interferograms measured simultaneously on opposite sides. Wringing the gauge block to a platen to form an optical step, as it is used in traditional gauge block comparators, is not required. In return, the influence of wavefront aberrations on the measured length is increased due to larger optical path lengths. A first idea for a correction method is presented in this paper.

## 1 Introduction

Prismatic bodies like gauge blocks, which are used to distribute the unit of the length to industry, are usually measured with single-ended interferometers like Twyman Green or gauge block comparators [1,2]. To get a reference for the position of the back face of the gauge block it has to be wrung to a platen to form an optical step which height represents the length as shown in figure 1a.

The measurement procedure using wrung gauge blocks is time-consuming, because both endfaces have to be wrung to a platen and be measured one after another, as the measured length is influenced by the wringing, dependent on the quality of the faces involved. Another problem is flexing of the platen, typically occurring when the temperature of the gauge block is different from the platen's temperature before being wrung together, which leads to errors in the measured gauge block length. So an alternative interferometer design is requested, in which the length of the gauge block or other prismatic bodies can be measured from both sides simultaneously, as shown in figure 1b, without the need for wringing.

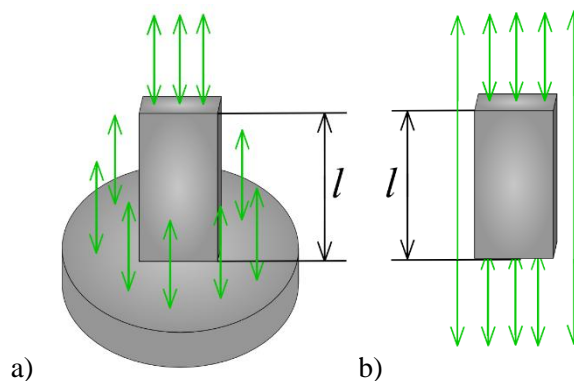


Figure 1: a) Step formed by wringing a gauge block to a platen for measuring the length in a single-ended interferometer, b) Gauge block length measured with a double-ended interferometer

Few years ago, a prototype double-ended interferometer based on the model of Kuriyama [3] was built at PTB to evaluate its functionality [4,5]. The ultimate double-ended interferometer is situated in a temperature-controlled vacuum chamber, uses optical components of higher quality and provides a larger beam diameter of 80 mm.

## 2 Experimental Setup

### 2.1 Layout of the interferometer

In contrast to the prototype [4,5], a shaken multimode fibre is used as light source to decrease parasitic interferences which have been identified and could not be removed in a different way. Light of two different iodine stabilized lasers, from a helium neon at 633 nm and a frequency doubled Nd:YAG laser at 532 nm, is coupled into the fibre, alternatively. A large collimated beam of 80 mm in diameter is formed by an achromatic lens with a focal length of 500 mm,  $L_1$ , at the fibre exit. This beam is split by a triangular configuration of wedged beamsplitter plates (CSIRO Materials Science and Engineering, Australia, Corning 7980-UV-0C Fused Silica,  $\frac{\lambda}{50}$ , wedge of  $10^\circ$ ) into two separated reference and imaging arms and a common measurement arm, in which the gauge block is placed (see figure 2). This allows measuring the gauge block from both sides at the same time without wringing the gauge block to a platen.

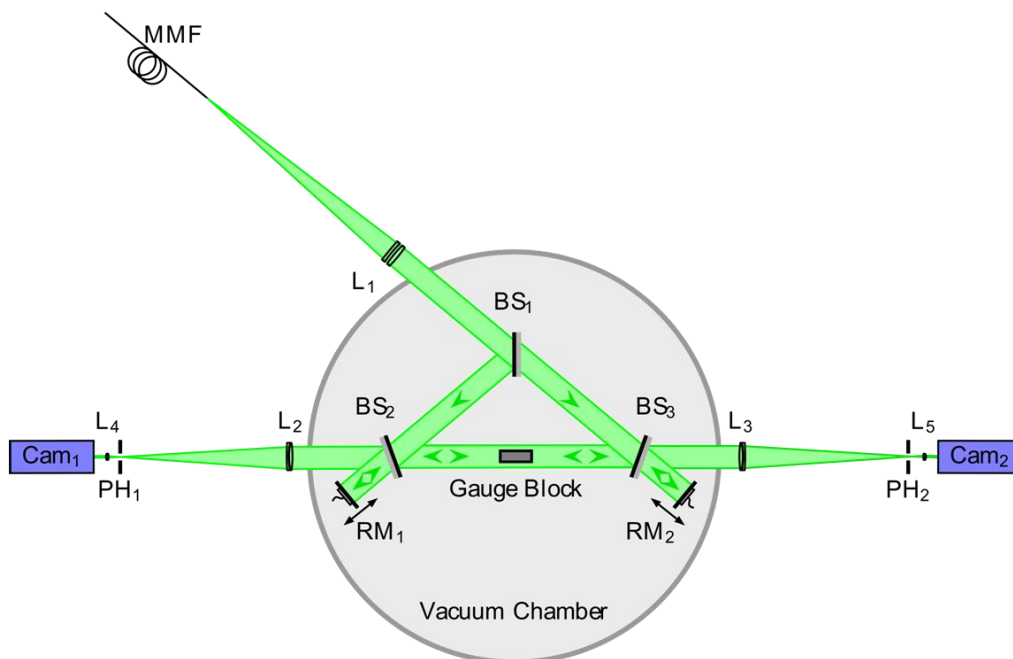


Figure 2: Setup of PTB's ultimate double-ended interferometer with shaken multimode fibre (MMF), wedged beamsplitter plates ( $BS_1, \dots, BS_3$ ), piezo-actuator controlled reference mirrors ( $RM_1, RM_2$ ), apertures ( $PH_1, PH_2$ ), achromatic lenses ( $L_1, \dots, L_5$ ) and CCD cameras ( $Cam_1, Cam_2$ )

In the reference arms, piezo-actuator controlled reference mirrors are used for phase-stepping interferometry. The two imaging arms are each equipped with an aperture, blocking unwanted reflections, achromatic lenses and a camera. To achieve ultimate stability, the interferometer is situated in a temperature-controlled vacuum chamber and the optical components are mounted on a triangle made of invar. To decrease vibrations, additional struts are used to interconnect the holders of the beamsplitter plates. The gauge block is positioned on a motorized sample table in the centre of the interferometer.

### 2.2 Stability of the interferometer

The first measurements related to the stability of the interferometer showed deviations from the mean length of several nm, released by vibrations in the interferometer [6]. Vibrations could be reduced considerably by installation of struts between the beamsplitter plate holders. Figure 3 demonstrates the performance by repeated length measurements on a silicon gauge block with nominal length of 15.046775 mm.

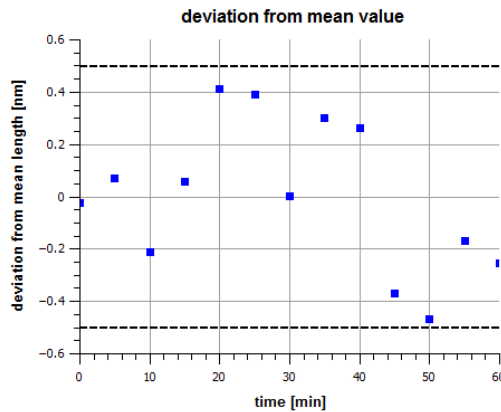


Figure 3: Deviation from mean length of a silicon gauge block over one hour

The deviation from the mean length lies well within  $\pm 0.5$  nm during one hour measurement time. This yields to a standard deviation of approximately 0.29 nm which represents a substantial progress compared to former stability measurements without the struts [6]. Residual vibrations are assumed to be generated by the closed loop stabilisation of one of the piezo actuators which was found to generate a back and forth tilt of the right reference mirror.

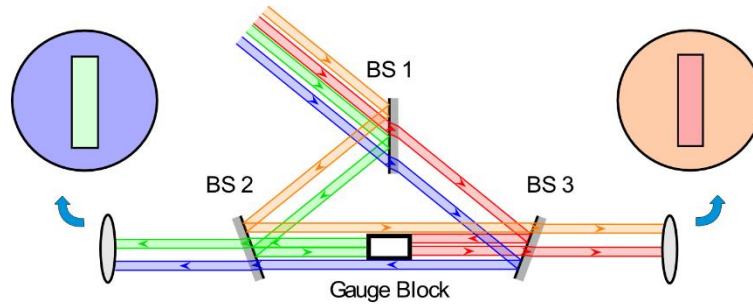
### 2.3 Alignment

To measure the actual length of the gauge block, the axis of the gauge block has to be parallel to the beam direction. Otherwise, i.e. if the sample is tilted with respect to the beam direction, the measured length is shorter than the actual length, initiated by the cosine error [7]. In a single-ended interferometer this can easily be assured by adjustment of the reference mirror and subsequent adjustment of the gauge block while observing the interference pattern until the fringes vanish as described in [8]. In a double-ended interferometer the beam alignment is more complicated. First it has to be guaranteed that the beam passing the gauge block from left to right is parallel to the one going from right to left. A tilt between them would yield to a measurement of the two gauge block faces from different angles and, therefore, cause an error of the measured gauge block length. Even if fluffed out interferograms are produced in both arms of the interferometer, it is not guaranteed that the beams incidents perpendicular to the faces of to the gauge block. To link the two interferometer arms to be parallel in the measurement path, a special alignment procedure of the interferometer is necessary. In a first step it is ensured, that the beam is perpendicular to the right reference mirror. This is done by tilting this mirror with the piezo actuators, while observing the amount of light retro-reflected into the multimode fibre at the entrance of the interferometer. In this approach the retro-reflected light is split from the reversely directed light by a fibre optical beam splitter and guided to a photo detector attached to the second end of the fibre optical beam splitter. By adjustment of the mirror to the maximum retro-reflection signal, a perpendicular incidence of the beam onto the mirror is guaranteed. In the next step, the left beamsplitter plate is tilted until the fringes in the interferogram of the right interferometer arm vanish. The left reference mirror is then tilted to produce a zero fringe interferogram in the left interferometer arm. By tilting the gauge block to get a fluffed-out interferogram in the right arm, the left arm is fluffed-out automatically, if the gauge block has parallel endfaces. In this way it is guaranteed that the beams coming from both sides are parallel to the length axis, so that the cosine error is minimized to a negligible level.

### 3 Length analysis

#### 3.1 Beam pathways

The length of the gauge block can be calculated by the difference of four separate path lengths which are indicated in figure 4.



$$l = \frac{1}{2}(P_1 - P_2 + P_3 - P_4) \quad (1)$$

Figure 4: four different pathways contributing to the length measurement

At the upper beamsplitter plate BS1, one half of the intensity of the light is reflected to the left beamsplitter plate BS2, the other half is transmitted to the right beamsplitter plate BS3. With these two beamsplitters the beam is directed to the center of the interferometer, where the inner part of the beam is reflected at the face of the gauge block, shown in figure 4 in green for the left side and in red for the right side. The outer part of the beam (shown in orange and in blue) passes along the gauge block to the other side of the interferometer. The circles indicate the beam cross section with a reference to the respective pathway. Accordingly, the length of the gauge block can be calculated by the difference of the optical path length of the beam passing along the gauge block to that reflected at the gauge block face, added up for both interferometer arms and divided by two (see equation 1). These optical path lengths are evaluated by interference analysis in the left and the right arm, as described in the next chapter.

#### 3.2 Phase analysis

Five phase shifted interferograms of each interferometer arm are recorded with the CCDs by using the piezo actuators to move the reference mirrors. A five-step phase algorithm by Tang [9] is used to calculate a phase-map which is shown in figure 5 together with the corresponding interferograms.

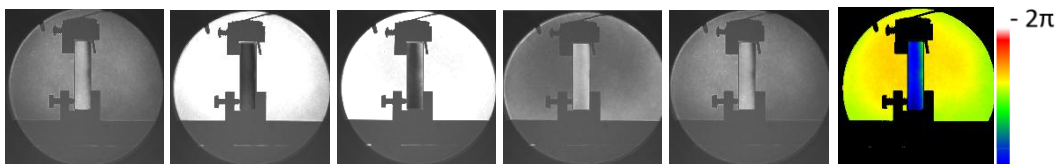


Figure 5: Five phase-shifted interferograms of right interferometer arm with resulting phase map

The difference in the optical path lengths is calculated using the phase difference of the outer part of the beam, which passes along the gauge block, to the inner part of the beam, which has been reflected at the gauge block face. The phase values are extracted out of several regions of interest shown in figure 6.

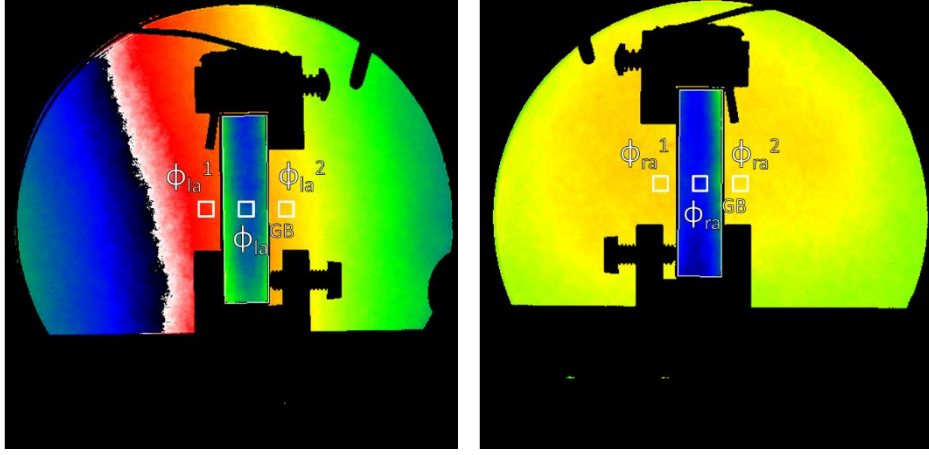


Figure 6: Phase maps with regions of interest of left and right interferometer arm

One region of interest is situated in the centre of the gauge block region, which position is determined by an edge detection algorithm. The two other regions of interest are arranged symmetrically around it outside the gauge block region. On the basis of the  $2\pi$  periodicity of the phase values, only the fractional order of interference  $q_k$  can be determined using the phase values of these regions of interest according to

$$q_k = \frac{1}{2\pi} \left\{ \left[ \frac{\Phi_{la}^1 + \Phi_{la}^2}{2} - \Phi_{la}^{GB} \right] + \left[ \frac{\Phi_{ra}^1 + \Phi_{ra}^2}{2} - \Phi_{ra}^{GB} \right] \right\} \quad (2)$$

To express the gauge block length by a multiple of the half wavelength, i.e.

$$l_k = \frac{\lambda_k}{2} (i_k + q_k), \quad (3)$$

the integer order of interference  $i_k$  has to be determined by applying the same measurement procedure with light from a second stabilized laser, which is coupled into the interferometer subsequently. For each wavelength the integer order  $i_k$  is varied individually and it is searched for coincidences in the resulting lengths for both wavelengths. This principle is called method of exact fractions [10]. The procedure applied in this paper is explained in detail in [11].

Since the measurement deals with the topography of the full gauge block faces, it is possible to analyse defects and deformations of the gauge block faces in addition to the length analysis. Besides the above mentioned advantages, compared to single ended interferometers, wavefront aberrations have a larger effect onto the measured length. This is caused by the longer pathways of the wavefronts.

#### 4 Influence of wavefront aberrations

While, under vacuum conditions, the effect of the refractive index of air to the length measurement is absent, other effects are limiting the uncertainty of the measured length, especially for the double-ended interferometer. One of the most challenging effects is the influence of wavefront aberrations on the measured length, which is demonstrated in this paper.

To get a first impression of the influence of wavefront aberrations on the measured length the simple case of spherical wavefronts is evaluated.

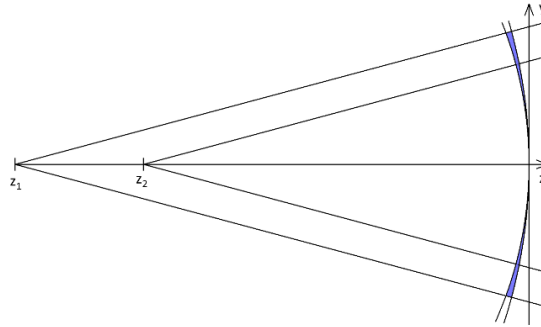


Figure 7: Propagation scheme of spherical wavefronts

Figure 7 shows a simplified propagation scheme of spherical wavefronts. In the interferometer several pathways with different optical path lengths are existent. This is comparable to different starting points of the wavefronts  $z_1$  and  $z_2$  compared to the plane of the camera  $y$ . Along the  $y$ -axis the wavefronts with different starting points exhibit distinct curvatures. The difference of these wavefront curvatures is shown as blue region in Figure 7. It leads to spherical shaped fringe systems on the camera and, subsequently, in bended phase topographies. Consequently, wavefront aberrations are directly influencing the measured length, especially when averaging over the two outer regions of interest which is necessary in the length evaluation (see equation 2). The size of this aberration induced length error can be investigated by theoretical considerations and studying the empty interferometer.

#### 4.1 Theoretical analysis by raytracing

The aberration induced length error is evaluated theoretically by a raytracing software. In this approach the wavefront propagation has to be calculated for six different pathways (two reference pathways, two pathways for reflection at the gauge block face and two pathways passing along the gauge block) considering the wedges in the beamsplitter plates and vacuum windows. Therefore, a self made raytracing program, written in C++, was modified for this interferometer. The software uses a high precision library to eliminate the influence of computational accuracy and offers the advantage of sequential raytracing combined with absolute positions of the optical components. This is of high importance to exactly superpose the different interferometer pathways, in particular the two measurement pathways from both sides. 15x15 rays are traced per pathway. Zernike polynomials are fitted to the optical path length at the incidence on the camera before calculating the interferograms. An automated alignment procedure was implemented for an easy test of different configurations. The influence of spherical wavefronts on the measured length was investigated by assuming a virtual displacement of the fibre from its ideal position, i.e. from the focal point distance for which the beam is ideally collimated. Large effects have been generated to test applicability of different correction methods. Figure 8 exemplarily shows theoretical results for the “virtual length measurement” with the raytracer for different fibre positions, assuming a gauge block length of 15.046 775 mm.

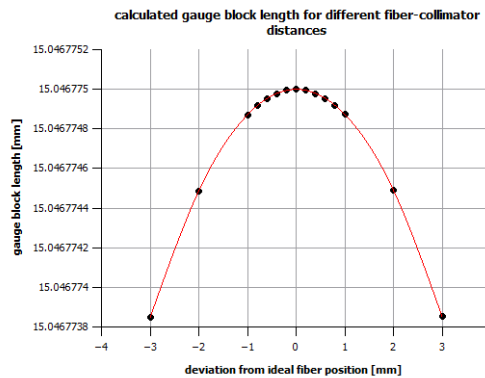


Figure 8: “Virtual length measurement” with the raytracer assuming several distances between fibre and collimator

As figure 8 reveals, the resulting gauge block length has a parabolic shape and exhibits a length error of nearly 1.2 nm for a deviation of the fibre from its ideal position of  $\pm 3$  mm.

#### 4.2 Correction of wavefront induced length errors by a raytracing of the empty interferometer

Figure 9a shows a phase map generated by raytracing with a deviation of the fibre from its ideal position of -3 mm. By passing the wedged vacuum windows and beamsplitter plates the incident spherical wavefront is then deformed to an elliptical shape. The problem of the bended wavefront is, nevertheless, existent.

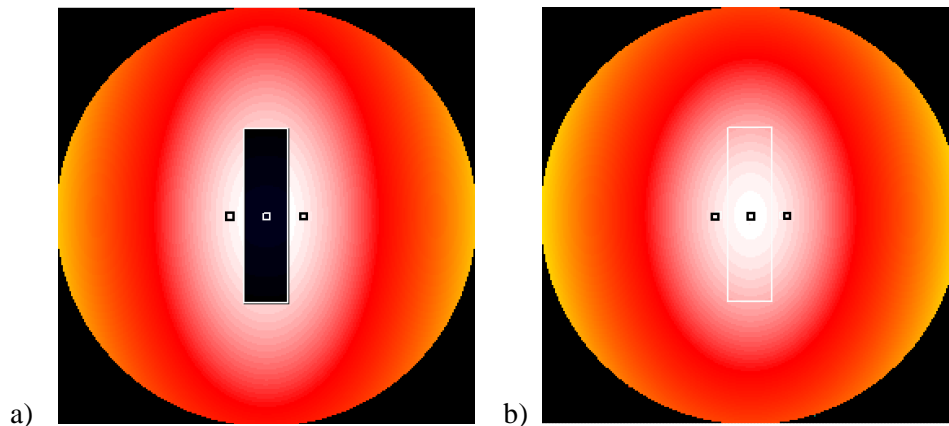


Figure 9: Phase map calculated from a raytracing with a deviation of the fibre position of -3 mm a) with gauge block, b) of the empty interferometer

To evaluate the bending of the wavefront and estimate the phase value in the center, which is usually covered by the gauge block, a raytracing of the empty interferometer is done. The resulting phase map is shown in figure 9b. The bending of the wavefront is then calculated by the phase difference of the same regions of interest as in the phase map with the gauge block. This phase difference, shown in figure 10a, is used as a first correction for the wavefront induced length errors in the “virtual length measurement”.

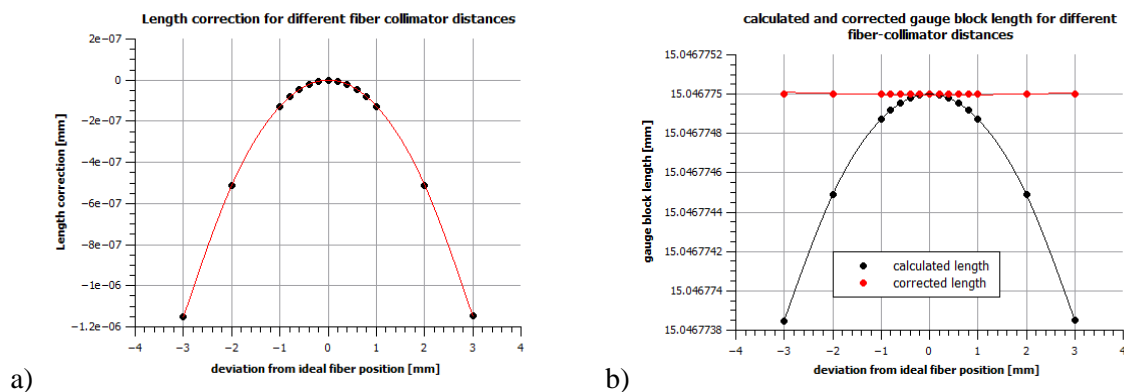


Figure 10: a) length correction obtained by raytracing of the empty interferometer b) gauge block length obtained with the raytracer and the corrected length using the raytracing of the empty interferometer

Figure 10 shows the result of the virtual length measurement with the raytracer with and without the correction. For the corrected values, coloured in red, the phase difference of the outer to the inner region of interest, obtained by the raytracing of the empty interferometer, was subtracted from the virtually measured gauge block length.

Consequently, the deviation in the calculated gauge block length for the range of fibre displacement of  $\pm 3$  mm could be decreased by three orders of magnitude by using the raytracing of the empty interferometer as a first correction for the wavefront aberration induced length errors.

### 4.3 Experimental results

Using the double ended interferometer, actual length measurements were performed under the same assumptions as the “virtual length measurements” described in section 4.1 and 4.2. Again the displacement of the fibre from its ideal position was used to create spherical wavefronts. The results of the measured lengths of a silicon gauge block with nominal length of 15.046 775 mm are shown in black in figure 11a.

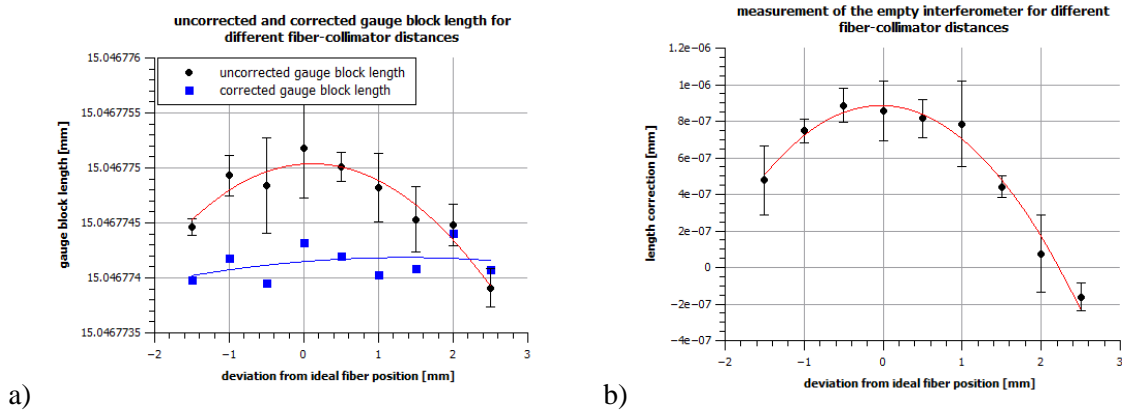


Figure 11: a) Experimental results for the measured gauge block length (black) for different fibre – collimator distances and corrected length (blue) using a measurement of the empty interferometer, b) measurement of the empty interferometer

The measured gauge block length shown in black has a similar distribution as the one obtained with the raytracer, but it exhibits a slightly larger length deviation of about 0.8 nm for a displacement of the fibre of  $\pm 2$  mm, compared to about 0.5 nm for the “virtual length measurement”.

The sample table can be shifted by using a motorised translation stage. This allows measurement of the empty interferometer just after measurement with the installed gauge block located in the central beam region. The results of measurement of the empty interferometer (shown in figure 11b) indicate a length deviation of about 0.7 nm for the range of fibre displacement of  $\pm 2$  mm. The peak of the length correction in figure 11b is shifted to 0.9 nm which differs from the results obtained by the raytracer. For perfectly plane waves this value is expected to be zero. This indicates that other sources for a bended wavefront are additionally effective, which might originate from imperfectness of the collimating lens, beamsplitter plates or reference mirrors.

As for the raytracing, this measurement can be used as a correction for the spherical wavefront induced length errors in the gauge block measurement. The resulting corrected gauge block length is shown in blue in figure 11a. The length deviation for a fibre displacement of  $\pm 2$  mm could be decreased to about 0.45 nm, which is in the range of the stability of the interferometer. So for wavefront aberrations induced by common optics of the beam passing along the gauge block and the beam reflected at the gauge block face, for example the entrance collimator, this correction method seems to be a promising way to reduce the effect of wavefront aberrations on the measured gauge block length.

However, for optic errors of the beamsplitter plates the correction by using the measurement of the empty interferometer does not necessarily work for the gauge block area. This is due to the crossing pathways of the beam passing along and the beam reflected at the gauge block, which are recorded on the same camera. It is noticed that the wavefront aberration can be quite different for the gauge block region as for the outer region. Another point is that, for different gauge block lengths, the pathways of the beams reflected on the gauge block face are variant. For this reason, the propagation of the wavefront errors varies with the gauge block length. Therefore, an additional correction for the wavefront errors in the gauge block region seems necessary, which accounts for the different optic errors compared to the outer part of the beam and for the different axial positions of the gauge block end faces.

## 5 Conclusion

PTB's ultimate double-ended interferometer enables absolute length measurement of prismatic bodies like gauge blocks without wringing them to a platen under vacuum and in air. Two different reference and imaging arms are used to measure the sample from both sides simultaneously. The actual stability of the measured length lies well within  $\pm 0.5$  nm within one hour. Since the influence of wavefront aberrations onto the length measurement is increased compared to single-ended interferometers, effective error corrections are necessary. Simulations by a raytracing software deliver insight in potential corrections. A correction for the outer part of the beam can be achieved by a phase measurement of the empty interferometer as shown by the raytracing and experimental results. For wavefront aberrations induced by the beamsplitter plates and for larger gauge block lengths an additional correction for the gauge block region seems necessary. More work is needed to obtain such correction, which is expected to be complex due to varying axial positions of the body's endfaces, dependent on the individual length of the body.

## References

- [1] Bönsch G 2001 Automatic gauge block measurements by phase-stepping interferometry with three laser wavelengths *Proc. SPIE* **4401** 1-10
- [2] Decker J E, Schödel R and Bönsch G 2003 Next generation Kösters Interferometer *Proc. SPIE* **5190** 14-23
- [3] Kuriyama Y, Yokoyama Y, Ishii Y and Ishikawa J 2006 Development of a new interferometric measurement system for determining the main characteristics of gauge blocks *Ann. CIRP* **55**
- [4] Abdelaty A, Walkov A, Abou-Zeid A and Schödel R 2010 PTB's Prototype of a Double-Ended Interferometer for Measuring the Length of Gauge Blocks *Symposium of metrology 2010-CENAM, Queretero, Mexico*
- [5] Abdelaty A, Walkov A, Franke P, Schödel R 2012 Challenges on double-ended gauge block interferometry unveiled by the study of a prototype at PTB *Metrologia* **49** 1-8
- [6] Rau K and Schödel R 2013 Double-ended interferometer for measuring gauge blocks without wringing *Fringe 2013, 7<sup>th</sup> international workshop on advanced optical imaging and metrology* 859-862
- [7] Bruce C F 1955 The effect of collimation and oblique incidence in length interferometers *Aust. J. Papers* **8** 224-240
- [8] Schödel R and Bönsch G 2004 Highest-accuracy interferometer alignment by retroreflection scanning *Applied Optics* **43** 5738-5743
- [9] Tang S 1991 Self-calibrating five-frame algorithm for phase shifting interferometry *Proc. SPIE* **2860** 91-98
- [10] Benoît J R 1898 Application des phénomènes d'interférence à des déterminations métrologiques *Phys. Radium* **7** 57-68
- [11] Schödel R 2015 Utilisation of coincidence criteria in absolute length measurements by optical interferometry in vacuum and air *MST* **101925** (to be published)